Journal of Physics: Conference Series **635** (2015) 012021 doi:10.1088/1742-6596/635/1/012021

Secondary ion emission from ethanol microdroplets induced by fast heavy ions

T Majima[1,2], K Kitajima[2], T Nishio[2], H Tsuchida[1,2] and A Itoh[1,2]

[1] Quantum Science and Engineering Center, Kyoto University, Uji 611-0011, Japan
[2] Department of Nuclear Engineering, Kyoto University, Kyoto 615-8540, Japan

E-mail: majima@nucleng.kyoto-u.ac.jp

Abstract. We have developed a new experimental setup that allowed us to study collision interactions between fast ions and liquid microdroplets under a high vacuum condition. Microdroplets of ethanol are irradiated with 1.0-MeV H^+ and 2.0-MeV C^{2+} ions. The size distribution of the droplets is evaluated from energy-loss measurements of projectile ions penetrating through the microdroplets. We obtain time-of-flight mass spectra of secondary ions from ethanol droplets. It is demonstrated that coincidence measurements with secondary electrons can distinguish specific ions produced in collisions with the droplets. Production mechanisms of H_3O^+, $C_4H_9O^+$, $(C_2H_5)_2OH^+$ in the liquid ethanol are discussed.

1. Introduction

Fundamental understanding of fast-ion induced processes in liquids is important in various fields such as biology, atmospheric science and nuclear engineering. Conventional experiments using liquid targets were limited mostly to irradiation under atmospheric pressure because of the high vapor pressure in vacuum. To open a new possibility to apply established techniques enabled in high vacuum conditions, we previously developed irradiation of liquid-jet targets with a MeV-energy ion beam. Mass-spectrometric studies were reported for secondary ions emitted from liquid-jet surfaces of ethanol, water and NaCl solutions [1,2].

Recently, we have developed a new experimental setup using microdroplets as an alternative liquid target to achieve ion-irradiation under a higher vacuum condition. This has a technical advantage in the sensitivity and resolution in mass spectrometry owing to less interference from background gases. In addition, new insights are expected by taking advantage of the properties of targets confined in a finite small size. Droplet experiments in vacuum have been already established in laser irradiation [3,4]. In particular, this has attracted much attention lately as a technique to offer macromolecular and nanocrystal targets for X-ray free-electron lasers [5,6]. However, irradiation of ion beams to liquid droplets are rare; one development was reported for spectroscopic studies with highly charged ion beams [7].

In this work, we report our first results of mass spectrometry of product ions obtained in collisions between a MeV-energy ion beam and microdroplets of the liquid ethanol C_2H_5OH (abbreviated to EtOH hereafter). We will discuss molecular processes generating some specific ion species initiated by a MeV-ion interaction in the liquid ethanol.

2. Experimental method

The experiment was performed using a 2 MV tandem type Pelletron accelerator at Quantum Science Engineering Center, Kyoto University. A schematic diagram of the experimental setup is shown in figure 1(a). Microdroplets of ethanol were generated by spontaneous Rayleigh breakup of a liquid jet [8,9]. The droplets were thus randomly injected. The liquid jet was prepared by the method proposed by Gañán-Calvo [8] as follows. A liquid ethanol (99.5 vol.%, Wako Pure Chemical Industries) was loaded into a pulled glass capillary at the flow rate of 0.05 ml/min by a HPLC Pump (LC-10AD, Shimadzu Corp.). An inner diameter of the capillary outlet was 58 μm. By putting the glass capillary close to an inlet of the vacuum chamber with a 200-μm diameter hole, we produced a thin liquid jet with a diameter of about 20 μm which is formed with a guide of a coaxial air flow into the vacuum chamber. Droplets thus produced were transported into a collision chamber through a differential pumping system as shown in figure 1(b). An aerodynamic lens [10] which consist of four apertures with diameters of 4.0–3.5 mm are placed before entering the first stage to make a confined beam and achieve better transmission of small droplets. The differential pumping stages are divided by a skimmer of 2-mm diameter and an aperture of 4-mm diameter. The droplets injected into the collision chamber were finally captured by a liquid nitrogen cold trap in the downstream. The vacuum pressures of the first stage, second stage and collision chamber were the order of 10^{1}, 10^{-2} and 10^{-4} Pa during the measurements.

Ion beams of 1.0-MeV H^{+} and 2.0-MeV C^{2+} ions were used for droplet-size measurements and secondary-ion mass spectrometry, respectively. To evaluate size distributions of the droplet targets at the collision region, distributions of the energy loss of incident H^{+} ions passing through droplets were measured by a solid state detector (SSD) with the active area of 25 mm^{2}. To avoid detection of enormous direct incident ions, forward-scattered ions were detected at a scattering angle θ of 34 ± 13 mrad.

Positive secondary ions ejected from droplet surfaces induced by collisions of 2.0-MeV C^{2+} ions were analyzed by a linear time-of-flight (TOF) mass spectrometer equipped with a microchannel plate (MCP) detector. TOF spectra were obtained by using a fast multichannel scaler (FMCS LN-6500, Labo.). In this experiments, two different trigger modes were employed. In the first mode, a pulsed ion beam of 20-ns width and 1-kHz repetition rate was prepared by a chopping deflector in the beam line. A synchronized signal with this pulsed ion beam was used for the start trigger of the FMCS. We call it hereafter “beam-chopping mode”. In the second mode called “electron-trigger mode”, on the other hand, a continuous ion beam was used. Secondary electrons emitted in the collisions were extracted to the opposite direction to the positive ions and detected by a secondary electron multiplier (Ceratron,

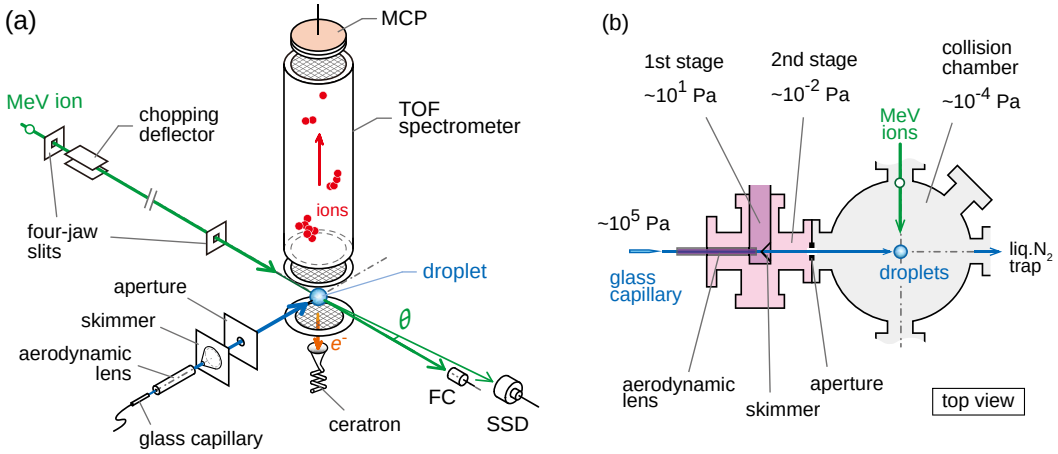

Figure 1. (a) Schematic diagram of the experimental setup, and (b) the differential pumping system to transport ethanol droplets into a high vacuum collision chamber.

Murata Corp.). The electron signals were used as the trigger in the electron-trigger mode. The signals from the Ceratron detector were on the order of tens to hundreds of mV and were fed to a constant fraction discriminator (CFD) before sending to the FMCS. In the present study, we compare two TOF spectra obtained with different threshold levels of the CFD, the "lower" setting at 50 mV and the "higher" setting at 90 mV, to distinguish product ions originating from the droplet target.

3. Results and discussion

Figure 2 shows energy spectra of forward-scattered ions observed at scattering angles θ of around 34 mrad for an incidence of 1.0-MeV H^+. An increased number of scattered ions are observed in a broad energy range when ethanol droplets are injected. They form a broad structure in the energy-loss distribution because the path length is different depending on the droplet size and the injection position in a droplet. Note that a sharp peak at 1.0 MeV is due to scattering with gas-phase molecules in the collision chamber and beam line. The vacuum pressure with and without the droplet target was about 5×10^{-4} and 2×10^{-4} Pa, respectively.

The top axis indicates the path length traveled in the ethanol, which is deduced from difference between the ranges at the injection energy (1.0 MeV) and at the outgoing energy. The range data were derived from SRIM2008 [11]. This provides evaluation of the size range of the droplets transported into the collision region. It was found that ethanol droplets have diameters ranging from a few to tens of micrometers. A detailed analysis, such as comparison with a Monte Carlo simulation, is required to obtain a precise size distribution of the droplets. It will be reported in a separate paper.

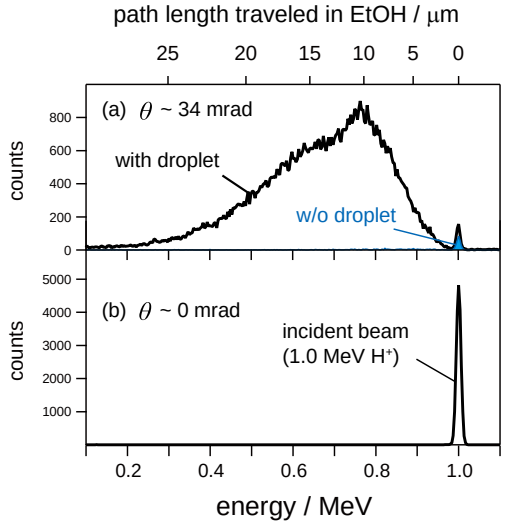

Figure 2. (a) Energy spectra of 1.0-MeV H^+ ions after scattering at around 34 mrad under the condition with and without ethanol droplet targets. (b) Energy spectrum of the incident beam of 1.0-MeV H^+ ions.

Figure 3 shows a TOF mass spectrum of secondary ions from ethanol droplets induced by 2.0-MeV C^{2+} ions, obtained in the beam-chopping mode. In the mass range smaller than $EtOH^+$, various fragment ions are observed as shown in figure 3(a). They can be assigned to $C_nH_m^+$, $C_nH_mO^+$ (n = 0–2, m = 1–3 for n = 0, m = 0–3 for n = 1 and m = 0–6 for n = 2) similar to previous studies with the liquid-jet target [1]. In addition to them, ions originating from the air, mainly nitrogen and oxygen, are involved in the present experiment since the droplets are delivered with a gas flow of the air. By replacing the carrier gas to simple one like helium, we can expect purification of the spectra for further quantitative analysis of the product ions in future experiments. Compared with the liquid-jet experiment, peak separation is improved owing to the lower vacuum pressure. The vacuum pressure at the liquid-jet experiment was worse by one order of magnitude than the present experiment; product ions were probably suffered from collisions with gas molecules during extraction in the TOF spectrometer. As we will show later, these small product ions, except for H_3O^+, are attributed predominantly to collision-induced dissociation of gas-phase molecules in the chamber. In the higher mass range, protonated ethanol cluster ions $(EtOH)_nH^+$ are observed up to $n \sim 8$. In the liquid-jet

experiment, it was observed that cluster ions are produced only when projectile ions hit the jet target. Thus, existence of these cluster ions clearly demonstrates that ion irradiation of microdroplets has been achieved in the present experiment. The intensity distribution of the cluster ions $(EtOH)_nH^+$ as a function of the size n is plotted in the inset of figure 3(b). The cluster intensities exhibit an exponentially decreasing behavior with n, as observed also in the liquid-jet experiment.

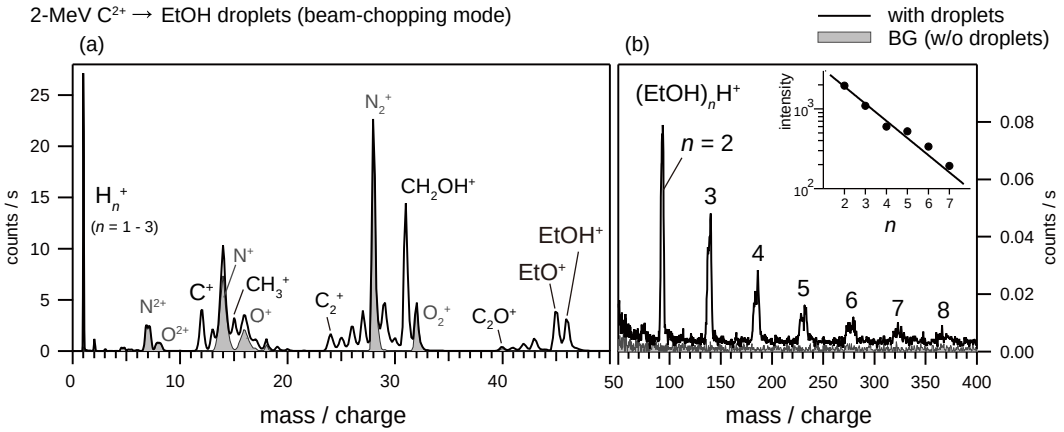

Figure 3. TOF mass spectrum of ions produced in collisions between 2.0-MeV C^{2+} ions and ethanol microdroplets, measured in the beam-chopping mode. The spectrum filled with gray color is the background spectrum without droplet targets. They are plotted separately in the two ranges of the mass-to-charge ratio of (a) 0–50 and (b) 50–400. Inset in (b) shows integrated peak intensities of protonated cluster ions $(EtOH)_nH^+$ as a function of the size n.

Figure 4 shows TOF mass spectra of secondary ions from ethanol droplets, obtained in the electron-trigger mode. We compare two spectra measured with the two different threshold levels (lower and higher) applied to signals of the secondary electrons. By setting the higher threshold, we can select collision events involving emission of a larger number of electrons. It is considered that collisions of a 2.0-MeV C^{2+} ion with microdroplets will cause emission of much larger number of electrons compared with collisions with gas-phase molecules. As a result, we can expect that product ions associated with gas-phase molecules are reduced more significantly by increasing the threshold level. In the present measurements, the total count rate of the electrons was reduced by about 5 times when we change the threshold level from the lower to higher setting.

Ion species observed in these spectra are almost identical to those obtained in the beam-chopping mode, except for their relative intensities in the TOF spectra. We see that peak intensities of product ions lighter than $EtOH^+$ drastically decrease at the higher threshold measurement, while intensities of clusters ions $(EtOH)_nH^+$ are almost unchanged. We also see that the baseline of the TOF spectra is reduced with increasing the threshold. As a result, peaks of the cluster ions become more prominent. It is found that the cluster peaks exhibit broad structure owing to their kinetic energies gained during the ion emission. A peak buried in the baseline at the mass-to-charge ratio (m/q) of about 75 also appears clearly.

The same spectra are shown in an expanded form in figure 4(b). The spectrum of the lower threshold is multiplied by 0.08 to compare the shapes of the spectra precisely in the smaller mass region. A peak of the protonated ethanol ion $(EtOH)H^+$ is now obviously observed at the higher threshold measurement, while it was hidden as a shoulder of the strong peak of $EtOH^+$ at the lower threshold measurement. The peak around m/q = 75 can be assigned to the protonated diethyl ether ion $(C_2H_5)_2OH^+$. This peak has a broad structure because of its kinetic energy as observed for the cluster ions. We can recognize the existence of $C_4H_9O^+$ ions at m/q = 73, by carefully analyzing the peak

structure. Observation of these two ion species of m/q = 75 and 73 were also reported in the study of product ions from an ethanol liquid-jet target by UV-multiphoton ionization [12]. In the range smaller than $EtOH^+$, the peak structures appear to be basically identical. But if we look carefully, we find that the peak of the hydronium ion H_3O^+ shows particular enhancement at the higher threshold measurement compared to the scaled spectrum of the lower threshold measurement.

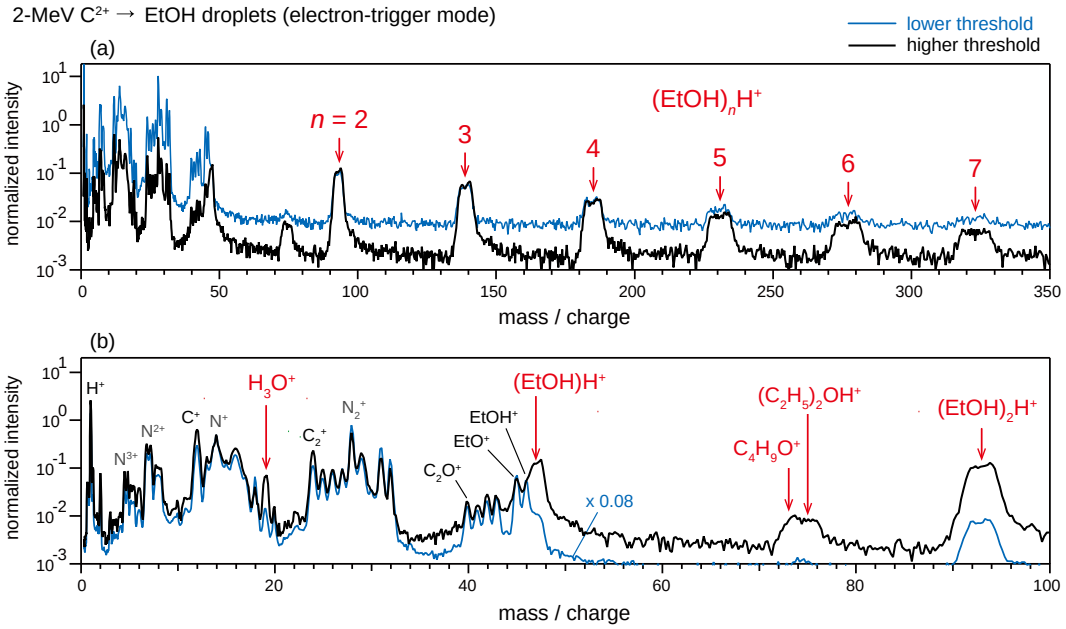

Figure 4. (a) TOF mass spectra of ions produced in collisions between 2.0-MeV C^{2+} ions and ethanol droplets, measured in the electron-trigger mode with two different threshold levels for the secondary electron detection, and (b) zoomed in the range of the mass-to-charge ratio less than 100. The intensities are normalized by the recoding time and the projectile beam current. In (b), intensity of the spectrum at the lower threshold is multiplied by 0.08 to make a comparison and clarify the difference between shapes of the two spectra.

Results shown in the last few paragraphs indicate that H_3O^+, $(C_2H_5)_2OH^+$ and $C_4H_9O^+$ ions, as well as the cluster ions $(EtOH)_nH^+$, are produced associated with collisions with droplet targets. Possible production mechanisms of the three ion species can be described as follows. To begin with, $EtOH^+$ ions are produced via ionization of ethanol molecules by projectile ions along their trajectories. It is suggested that $C_2H_5O^+$ (abbreviated to EtO^+) ions are also produced associated with ionization processes [13]. These ions immediately react with neighboring molecules and generate protonated ethanol ions $(EtOH)H^+$ as follows [13–15]:

$$EtOH^+ + EtOH \rightarrow (EtOH)H^+ + EtO\,, \tag{1}$$

$$EtO^+ + EtOH \rightarrow (EtOH)H^+ + CH_3CHO\,. \tag{2}$$

It is reported that $(EtOH)H^+$ ions decompose as follows at temperatures higher than 600 K [17]:

$$(EtOH)H^+ \rightarrow H_3O^+ + C_2H_4\,, \tag{3}$$

$$(EtOH)H^+ \rightarrow EtO^+ + H_2\,. \tag{4}$$

In the liquid phase, further reactions can proceed between $(EtOH)H^+$ and neighboring EtOH molecules. Protonated diethyl ether ions $(C_2H_5)_2OH^+$ will be produced through the following reaction [17]:

$$(EtOH)H^+ + EtOH \rightarrow (C_2H_5)_2OH^+ + H_2O\,. \quad (5)$$

In addition, production of $C_4H_9O^+$ is explained by the following two pathways as also reported in [17]:

$$(C_2H_5)_2OH^+ \rightarrow C_4H_9O^+ + H_2\,, \quad (6)$$

$$EtO^+ + EtOH \rightarrow C_4H_9O^+ + H_2O\,. \quad (7)$$

Although the reaction (4) indicates production of EtO^+ ions, they might be depleted through the reactions (2) and (7) immediately. The above reaction scheme reasonably explains the production of H_3O^+, $(C_2H_5)_2OH^+$ and $C_4H_9O^+$ ions followed by a fast ion collision in an ethanol droplet.

4. Summary

We demonstrated collision experiments between MeV-energy ion beams and ethanol microdroplets in a high vacuum condition. The size range of the droplet targets were obtained from energy-loss spectra of forward-scattered ions. We performed a mass-spectroscopic study of positive secondary ions from ethanol microdroplets. We revealed product ions specific to reactions in the ethanol liquid target with the help of coincidence measurements with secondary ions.

Acknowledgments

We gratefully acknowledge Dr J. Kohno for his advice on the liquid droplet technique. One of the authors (T.M.) would like to acknowledge the support of Toyota Physical & Chemical Research Institute Scholars and Kansai Research Foundation for Technology Promotion. We also acknowledge Mr. M. Naito, Y. Sasaki, Y. Oonishi and H. Ueda for his technical support during the experiment.

References

[1] Kaneda M, Shimizu M, Hayakawa T, Iriki Y, Tsuchida H and Itoh A 2010 *J. Chem. Phys.* **132** 144502,
[2] Kaneda M, Shimizu M, Hayakawa T, Nishimura A, Iriki Y, Tsuchida H, Imai M, Shibata H and Itoh A 2009 *Nucl. Instr. and Meth. In Phys. Res.* B **267** 908
[3] Morgner N, Barth H-D and Brutschy B, 2006 *Aust. J. Chem.* **59** 109
[4] Kohno J, Toyama N and Kondow T, 2006 *Chem. Phys. Lett.* **420** 146
[5] Chapman H N et al., 2011 *Nature* **470** 73.
[6] Kirian R A et al., 2015 *Struct. Dyn.* **2** 041717
[7] Padmashree G K, Roy A, Kanjilal D, Rodrigues G, Ahuja R, Somashekar R and Safvan C P, 2004 *Rev. Sci. Instrum.* **75** 5094
[8] Gañán-Calvo A 1998 *Phys. Rev. Lett.* **80** 285
[9] DePonte D P, Weierstall U, Schmidt K, Warner J, Starodub D, Spence J C H and Doak R B 2008 *J. Phys. D. Appl. Phys.* **41** 195505
[10] Liu P, Ziemann P J, Kittelson D B and McMurry P H 1995 *Aerosol Sci. Technol.* **22** 293, Liu P, Ziemann P J, Kittelson D B and McMurry P H 1995 *Aerosol Sci. Technol.* **22** 314
[11] Ziegler J F, Biersack J P and Ziegler M D, SRIM 2008, available from http://www.srim.org.
[12] Mafuné F, Kohno J and Kondow T 1996 *J. Phys. Chem.* **100** 10041
[13] Myron J J J and Freeman G R 1965 *Can. J. Chem.* **43** 381
[14] Ryan K R, Sieck L W and Futrell J H 1964 *J. Chem. Phys.* **41** 111
[15] Myron J J J and Freeman G R 1965 *Can. J. Chem.* **43** 1484
[16] Sieck L W, Abramson F P and Futrell J H 1966 *J. Chem. Phys.* **45** 2859
[17] Meot-ner (Mautner) M and Sieck L W 1989 *Int. J. Mass Spectrom. Ion Process.* **92** 123